nzsee
NEW ZEALAND SOCIETY FOR EARTHQUAKE ENGINEERING

A displacement-based design method for low-damage dual systems with hysteretic and nonlinear viscous energy dissipation

A. Gu, G.W. Rodgers
Department of Mechanical Engineering, University of Canterbury, Christchurch.

R.S. Henry
Department of Civil and Environmental Engineering, University of Auckland, Auckland.

ABSTRACT

In 2019, a large shaking-table test was performed for a full-scale two-storey low-damage concrete wall building. The test building comprises unbonded post-tensioning (UPT) rocking walls and perimeter frames in both directions. The perimeter frames incorporated hysteretic energy dissipation devices at slotted-beam connections at the beam-column and beam-wall joints, so that both UPT walls and perimeter frames would resist seismic action in parallel as a low-damage dual system. High force-to-volume (HF2V) lead-extrusion dampers and nonlinear viscous dampers (NVDs) were adopted in the test building.

This experimental test building was used as the basis for a parametric computational study in *OpenSees*, where a range of structural parameters were modified, including number of stories, wall-strength contribution ratios, effective period, and equivalent damping ratio. A displacement-based design method is proposed for the application of the low-damage dual system with energy dissipating device combination and compared against the computational results. Nonlinear time-history analyses (NLTHAs) were conducted to validate the methodology, and key response parameters from the time-histories are compared with the design values, to validate the proposed displacement-based design process.

The global responses of the NLTHAs validated the proposed design process for both coupled and decoupled dual systems, with the average absolute relative error of the roof drift being 7.94%, considering NVDs' EVD determined by the power approach. However, the proposed design process

was shown to significantly underestimate the roof drift responses of the decoupled dual system when the wall strength portion was smaller than 0.7.

1 INTRODUCTION

In 2019, a large shaking-table test was performed for a full-scale two-storey low-damage concrete wall building (Henry et al. 2020 & 2021, Lu 2020), as shown in Figure 1. The test building under D1b configuration incorporated HF2V devices (Rodgers 2009) and NVDs (Golzar et al. 2018) to enhance the energy dissipating ability of the test building. Despite having some velocity dependence in their response behaviour, the HF2V devices can be approximately modelled as displacement-based energy dissipators with a simple hysteretic response, given that the HF2V devices are relatively insensitive to velocity, with a velocity exponent of approximately 0.12 (Rodgers et al. 2008a & 2008b).

The NVD devices were velocity-dependent energy dissipations with velocity exponents of approximately 0.3. Coupled and decoupled low-damage dual systems were considered in the longitudinal and transverse directions of the test building, respectively. Specifically, the UPT walls were coupled to the floors via a flexible link-slab in the longitudinal direction, while the UPT walls were vertically decoupled from the floors in the transverse direction via a tongue that transfers only horizontal shear forces.

A displacement-based design method was proposed for the application of the low-damage dual system with the D1b energy dissipation device combination. NLTHAs were conducted to validate the methodology, and key response parameters from the NLTHAs are compared with the design values to validate the proposed displacement-based design process.

2 THE PROPOSED DISPLACEMENT-BASED DESIGN PROCESS FOR THE LOW-DAMAGE DUAL SYSTEMS

2.1 The configuration of the low-damage dual system

The low-damage dual systems, which were adopted in the test building under the D1b configuration, are shown in Figure 1. The HF2V devices were installed at the bottom of the slotted-beam joints while the NVD dampers were installed at the UPT wall base to increase the damping level of the system, as presented in Figure 1. The detailed design information of the test building is presented in Henry et al (2021).

As noted earlier, depending on different beam-to-wall connections, the low-damage dual systems could be categorised as coupled dual systems, or decoupled dual systems. In the longitudinal direction of the test building (Fig. 1a), the beam ends were directly connected to the UPT wall edges and linked into the floors via a flexible link-slab, so this kind of dual system was regarded as a coupled dual system. In the transverse direction of the test building (Fig. 1b), the frame was separated from the UPT wall uplift by the isolating connection that transferred only horizontal shear but allowed relative motion vertically, so this kind of dual system was regarded as a decoupled dual system.

The coupled dual system should consider the additional moment developed in the wall from floor interaction effects (Gu et al, 2022), so the wall and frame moment calculations at each storey would be different compared with the decoupled dual system. A framing effect parameter $\varphi_{framing}$ was considered for the coupled dual system to account the influence of the wall length on the beam moment assignment. The $\varphi_{framing}$ parameter also represented the ratio of the beam moment M_{j2w} developed at wall centreline and the beam moment M_{j2c} at the column centreline.

$$\varphi_{framing} = \frac{M_{j2w}}{M_{j2c}} \quad (1)$$

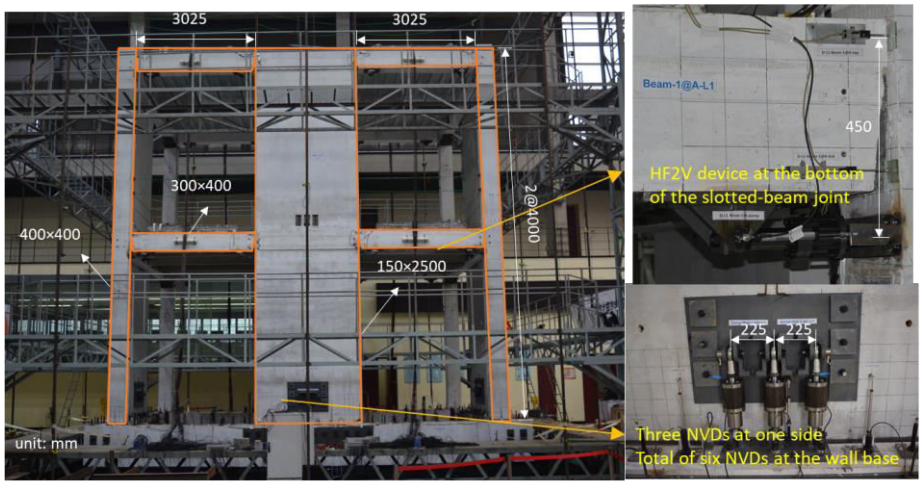

(a) Coupled wall-frame system in longitudinal direction

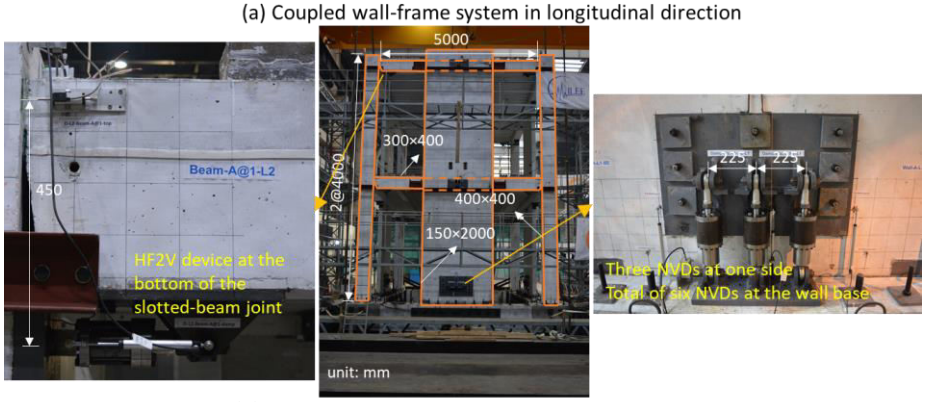

(b) Decoupled wall-frame system in transverse direction

Figure 1: Dual systems in the D1b test building

2.2 The displacement-based design process

Figure 2 presents the flowchart of the proposed displacement-based design process. The objective of the process is to design a structure that could meet the target displacement at peak response (Priestley 2002). The corresponding yielding displacement and design displacement profiles of the structure need to be determined to convert the multiple degree-of-freedom (MDOF) system to the equivalent single degree-of-freedom (SDOF) system. The capacity demand C_d was determined by the Equivalent Viscous Damping (EVD) ratio calculated for the structure and the damped design spectrum.

The estimation of the EVD ratio of the structural system was an important step in this process (Blandon 2005). The hysteretic responses of the HF2V devices were represented by a bilinear hysteretic response. The local hysteretic EVD of the HF2V devices was determined based on the Jacobsen approach (Jacobsen 1930 & 1960) in the proposed design process. Then, the local hysteretic EVD was transformed to the global level proportioned to the moment contribution from the HF2V devices. This transformation was undertaken because the energy absorption of the self-centring structure was influenced by the ratio of the hysteretic energy dissipations moments and the self-centring moments (Christopoulos et al. 2002).

Peckan et al. (1999) proposed a converting equation to consider the actual velocity spectra from the pseudo-velocity spectra, and an equation to determine the EVD of the NVDs, based on the SDOF structural system. The equations proposed by Peckan et al. were adopted for the NVDs' EVD determination in the proposed design process of the low-damage dual system. Energy and power approaches of the NVDs' EVD determination were considered in the proposed design process. The local NVD properties c_{nvd} were transformed from the global NVD properties by equating the energy dissipation.

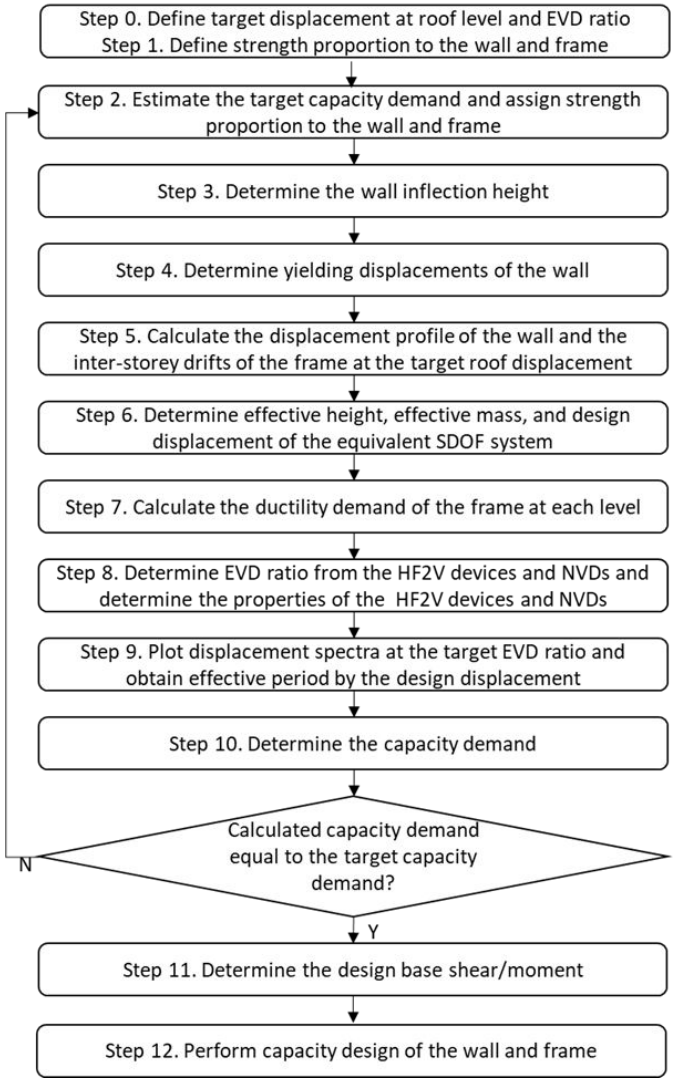

Figure 2: Flowchart of the proposed displacement-based design process

3 VALIDATION OF THE PROPOSED DISPLACEMENT-BASED DESIGN PROCESS

3.1 Structural models designed by the proposed design process

A total of 16 structural models were determined by the proposed design process and considering three design parameters: 1) wall strength portion φ_{wall}, 2) nonlinear velocity exponent of NVDs, α, and 3) total number of stories, n. The storey heights of all the structural models were set to be the same and had a value of 4 m. The cross sections of the columns and beams were 400 mm × 400 mm and 300 mm × 400 mm for all the structural models. The column spacing of all the structural models representing the coupled dual systems was 8950 mm, while the column spacing of all the structural models representing the decoupled dual systems was 5400 mm. The seismic mass of the roof level in all the structural models was 18.2 tonne, while the seismic mass of other levels in all the structural models was 26.6 tonne.

The target roof drift, which was 1%, remained the same for all the structural models. The 150% and 125% seismic demand spectra were adopted for the structural models of the coupled and decoupled dual systems, respectively. The seismic demand spectra were the design spectra of the D1b test building (Henry et al. 2021). The total EVD ratios of the coupled and decoupled dual systems were 30% and 25%, respectively.

The unconfined/confined concrete and the PT bar properties were derived from the low-damage dual systems in the D1b test building. Energy and power approaches of the NVDs' EVD ratio determination were considered for each structural model. The structural models designed based on the proposed design process are summarised in Tables 1 and 2.

Table 1: Design results of the structural models representing the coupled dual systems

Model number			**1-C**	**2-C**	**3-C**	**4-C**	**5-C**	**6-C**	**7-C**	**8-C**
Target C_d (g)			0.427	0.3	0.216	0.427	0.427	0.427	0.427	0.427
φ_{wall}			0.67	0.67	0.67	0.6	0.75	0.67	0.67	0.67
$\varphi_{framing}$			1.78	1.78	2.28	1.78	1.78	1.78	1.78	1.78
Equivalent SDOF system	T_{eff} (s)		0.77	1.23	2	0.77	0.77	0.77	0.77	0.77
	S_d (mm)		63	114	218	63	63	63	63	63
	C_d (g)		0.432	0.303	0.219	0.433	0.433	0.432	0.432	0.432
Wall	Wall length L_w (m)		2.5	2.5	3.5	2.5	2.5	2.5	2.5	2.5
	Wall thickness t_w (mm)		150	300	450	150	150	150	150	150
	c/L_w *		0.036	0.046	0.044	0.033	0.041	0.036	0.036	0.036
HF2V	$F_{HF2V,y}$ (kN)		69	88	102	84	52	69	69	69
	$\theta_{joint,y}$(%)		0.17	0.17	0.17	0.17	0.17	0.17	0.17	0.17
	r		0							
	ξ_{hys} (%)		18.1	18	18.4	22	13.8	18.1	18.1	18.1
NVD	α		0.35	0.35	0.35	0.35	0.35	0.5	0.75	1
	ε	EN	0.09	0.06	0.05	0.06	0.14	0.11	0.13	0.17
		PO	0.07	0.05	0.04	0.04	0.1	0.09	0.12	0.17
	c_{nvd}(kN·s$^{\alpha}$/mm$^{\alpha}$)	EN	32	99	224	19	47	17	6	2
		PO	25	76	172	15	36	14	5	2
	$\xi_{supplementary}$ (%)		9.9	10	9.6	6	14.2	9.9	9.9	9.9
PT bars**	n_{PT}		1	3	3	1	1	1	1	1
	$d_{PT,interval}$ (mm)		N.A.	150	150	N.A.	N.A.	N.A.	N.A.	N.A.
	A_{PT} (mm^2)		490.9	490.9	1017.9	415.5	572.6	490.9	490.9	490.9
	$f_{PT,initial}$ (MPa)		685.8	669.6	454.7	698	681.5	685.8	685.8	685.8
Base moment M_{total} (kN·m)			1066	2740	7574	1066	1066	1066	1066	1066
Ψ			0.022	0.034	0.032	0.02	0.025	0.022	0.022	0.022
T_i (s)			0.16	0.36	0.64	0.15	0.16	0.16	0.16	0.16

*The neutral axis depth ratio is calculated at the target roof drift.

** PT bars were arranged at the wall centreline.

Table 2: Design results of the structural models representing the decoupled dual systems

Model number			1	2	3	4	5	6	7	8
Target C_d (g)			0.352	0.246	0.184	0.352	0.352	0.352	0.352	0.352
φ_{wall}			0.79	0.79	0.79	0.6	0.7	0.79	0.79	0.79
$\varphi_{framing}$			0							
Equivalent SDOF system	T_{eff} (s)		0.85	1.36	2.19	0.85	0.85	0.85	0.85	0.85
	S_d (mm)		63	114	218	63	63	63	63	63
	C_d (g)		0.352	0.246	0.184	0.352	0.352	0.352	0.352	0.352
Wall	Wall length L_w (m)		2	2.5	3.5	2	2	2	2	2
	Wall thickness t_w (mm)		150	300	450	150	150	150	150	150
	c/L_w		0.04	0.05	0.05	0.05	0.06	0.04	0.04	0.04
HF2V	$F_{HF2V,y}$ (kN)		101	130	185	192	144	101	101	101
	$\theta_{joint,y}$(%)		0.18	0.18	0.2	0.21	0.18	0.18	0.18	0.18
	r		0							
	ξ_{hys} (%)		11	10.8	10.5	17	15	11	11	11
NVD	α		0.267	0.267	0.267	0.267	0.267	0.5	0.75	1
	ε	0.1	0.07	0.05	0.05	0.07	0.12	0.15	0.2	0.17
		0.07	0.05	0.04	0.04	0.05	0.1	0.14	0.2	0.17
	c_{nvd}(kN·s$^{\alpha}$/mm$^{\alpha}$)	73	165	373	38	50	29	11	4	2
		55	123	278	28	37	24	10	4	2
	$\xi_{supplementary}$ (%)		13	13.2	13.5	7	9	13	13	13
PT bars	n_{PT}		2	3	3	2	2	2	2	2
	$d_{PT,interval}$ (mm)		430	215	215	430	430	430	430	430
	A_{PT} (mm^2)		490.9	660.5	1017.9	346.4	415.5	490.9	490.9	490.9
	$f_{PT,initial}$ (MPa)		475.2	464.4	479.5	473	482.8	475.2	475.2	475.2
Base moment M_{total} (kN·m)			1066	866	2229	6350	866	866	866	866
Ψ			0.022	182	468	1332	346	260	182	182
T_i (s)			0.16	684	1761	5018	520	606	684	684

3.2 Nonlinear Time-History Analysis (NLTHA) results

The ground motions were selected for each structural model considering the interest period range from T_i to T_{eff}. The global responses from the NLTHAs were compared with the design values. The ground motion selection method was based on NZS 1170.5 (2004). Since different intensities and different total number of stories were considered in the models, the ground motions were selected for each structural model separately. A suite of 20 ground motions, with minimum mean square difference for each structural model, were selected. The selected ground motion records for structural models with different total storey numbers were presented in Figure 3, and the selected ground motion records were from the PEER database (Ancheta et al. 2014).

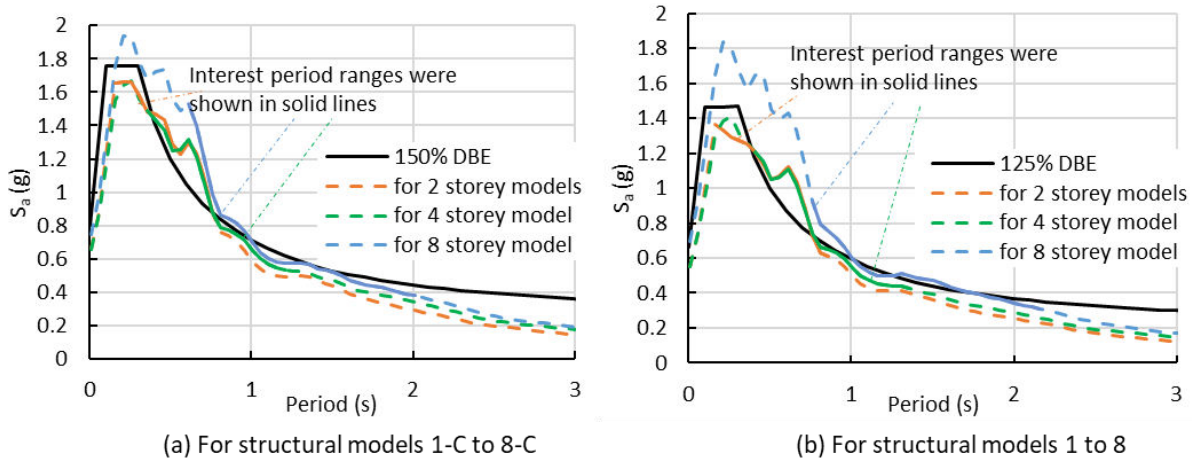

Figure 3: Overlay of the response spectra for the selected ground motions with the corresponding code-based design spectrum.

The computational models to represent each of the structural design cases were established in *OpenSees* to perform the NLTHAs. Figures 4 and 5 have shown the statistical global responses of the analytical models considering coupled and decoupled dual systems. The global responses of the analytical models were represented by the arithmetic sample mean of the NLTHAs.

As shown in Figures 4a and 5a, the roof drifts of all the models except models 4 and 5 were below or align to the target roof drift. The roof drift responses of NLTHAs tend to decrease with the increasing of the total number of stories, and the roof drift responses of NLTHAs tend to decrease as the wall strength portion is decreased. The roof drift responses of NLTHAs would increase as the nonlinear velocity exponent of the NVDs increases towards 1.0, when the NVDs' EVD was determined by the energy approach. The roof drift responses of the models with NVDs' EVD ratio determined by power approach were larger than those of the models with NVDs' EVD determined by energy approach as shown in Figures 4a and 5a.

The roof drift responses of the models designed as coupled dual systems were relative smaller than those of the models designed as decoupled dual systems. The C_d at peak roof drift all aligned to the target values for all models as shown in Figures 4b and 5b, while the $C_{d\,max}$ would exceed the target capacity demand due to the existence of the NVDs as shown in Figures 4c and 5c. The global responses of the models have confirmed that the proposed design process is appropriate, with the average absolute relative error of the roof drift being 7.94% considering NVDs' EVD determined by the power approach. However, the proposed design process would significantly underestimate the roof drift responses of the decoupled dual system when the wall strength portion is smaller than 0.7.

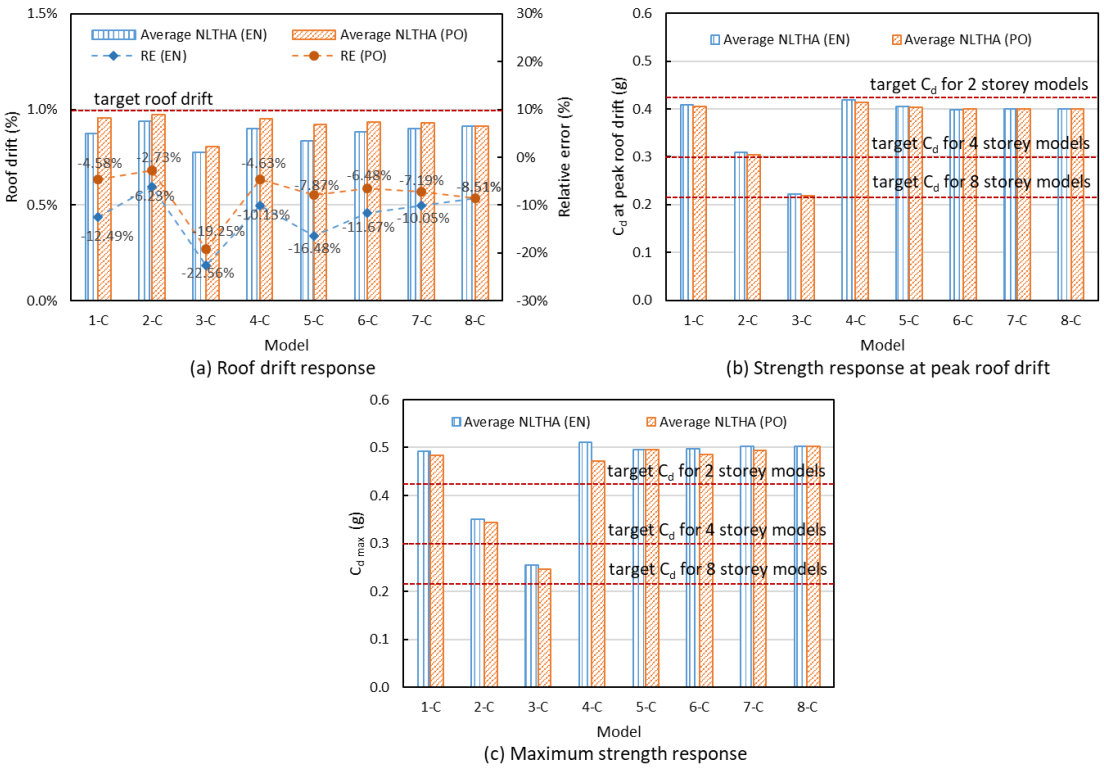

Figure 4: Global responses of models 1-C to 8-C designed as coupled dual systems

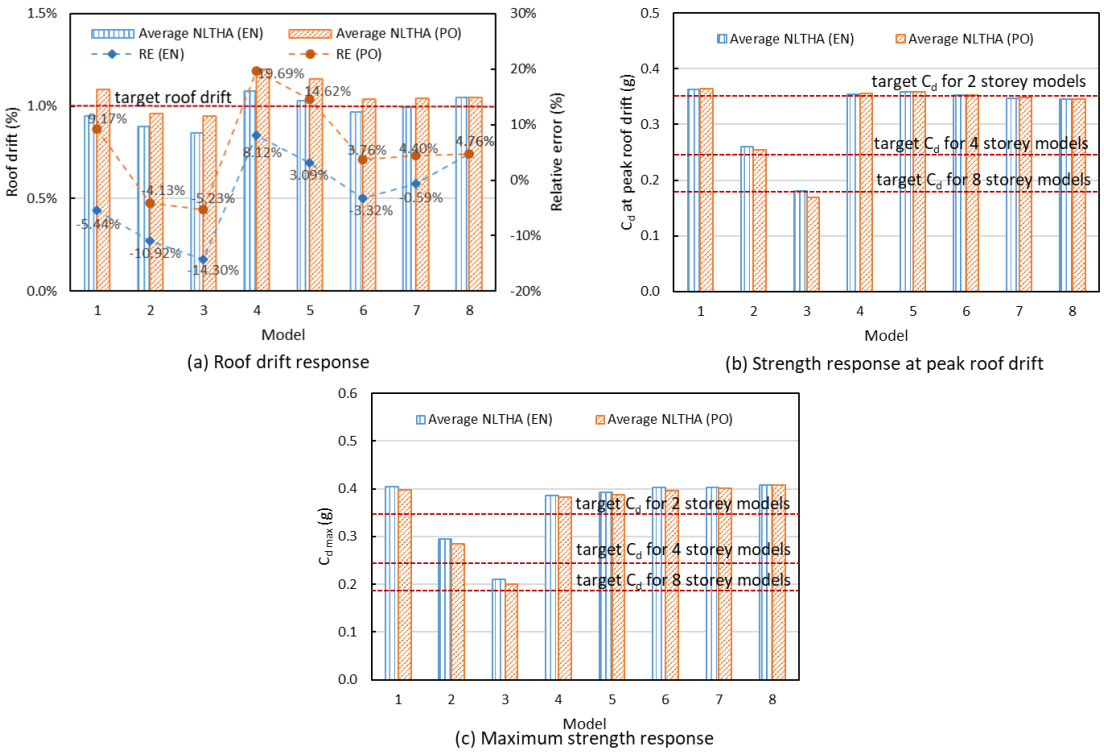

Figure 5: Global responses of models 1 to 8 designed as decoupled dual systems

4 CONCLUSIONS

The low-damage dual systems derived from the experimental test building under the D1b design configuration were studied, and the corresponding design process was proposed. The low-damage dual systems include coupled and decoupled dual systems, and two different methods for the NVDs' EVD ratio were considered in the proposed design process. A total of 16 low-damage dual systems were designed, based on this design process considering three design parameters: 1) wall strength portion, 2) nonlinear component of NVDs and 3) total number of stories. Finite element models were established in *OpenSees* to represent each of the structural models. NLTHAs were conducted to validate this design process. The global responses of the NLTHAs validated the proposed design process for both coupled and decoupled dual systems, with the average absolute relative error of the roof drift being 7.94%, considering NVDs' EVD determined by the power approach. However, the proposed design process was shown to significantly underestimate the roof drift responses of the decoupled dual system when the wall strength portion was smaller than 0.7.

ACKNOWLEDGEMENTS

The authors wish to acknowledge financial support provided by International Joint Research Laboratory of Earthquake Engineering (Grant No. ILEE-IJRP-P2-P4-2017), the New Zealand Ministry of Business, Innovation and Employment (MBIE) Building System Performance, a Royal Society Te Apārangi Rutherford Discovery Fellowship, and QuakeCoRE, a New Zealand Tertiary Education Commission-funded Centre.

REFERENCES

Ancheta TD, Darragh RB, Stewart JP, Seyhan E, Silva WJ, Chiou BSJ, Wooddell KE, Graves RW, Kottke AR, Boore DM, Kishida T and Donahue JL. (2014). "NGA-West2 database". *Earthquake Spectra*, **30**(3): 989-1005. DOI: 10.1193/070913EQS197M

Blandon CA, and Priestley MJN. (2005). "Equivalent viscous damping equations for direct displacement-based design". *Journal of earthquake Engineering*, **9**: 257-278. DOI: 10.1142/S1363246905002390

Christopoulos C, Filiatrault A and Folz B. (2002). "Seismic response of self-centring hysteretic SDOF systems". *Earthquake engineering & structural dynamics*, **31**(5):1131-1150. DOI: 10.1002/eqe.152

Golzar FG, Rodgers GW and Chase JG. (2018). "Design and experimental validation of a re-centring viscous dissipater". *Structures*, **13**: 193-200. DOI: 10.1016/j.istruc.2017.12.008

Gu A, Zhou Y, Henry RS, Lu Y and Rodgers GW. (2022). "Simulation of shake-table test for a two-story low-damage concrete wall building". *Structural Control and Health Monitoring*, **29**(10). DOI: 10.1002/stc.3038

Henry RS, Lu Y, Zhou Y, Lu Y, Rodgers GW, Gu A, Elwood KJ and Yang T. (2020). "Dataset on shake table test of a low-damage concrete wall building". *DesignSafe-CI*. DOI: 10.17603/ds2-ncac-sg36

Henry RS, Zhou Y, Lu Y, Rodgers GW, Gu A, Yang Q, Elwood KJ and Yang T. (2021). "Shake-table test of a 2-storey low-damage concrete wall building". *Earthquake engineering & structural dynamics,* **51**(12): 3160-3183. DOI: 10.1002/eqe.3504

Jacobsen LS. (1930). "Steady forced vibration as influenced by damping". *Transactions of ASME*, **52**(15): 169-181.

Jacobsen LS. (1960). "Damping in composite structures". *Proceedings of the 2nd world conference on earthquake engineering*, Japan: Tokyo.

Lu Y, Henry RS, Zhou Y, Rodgers GW, Yang Q and Gu A. (2022). "Data set for a shake-table test of a 2-story low-damage concrete wall building". *ASCE Journal of Structural Engineering*, **148**(7): 04722002. DOI: 10.1061/(ASCE)ST.1943-541X.0003348.

Standards New Zealand (2004). "*NZS1170.5: Structural Design Actions. Part 5: Earthquake Actions - New Zealand"*. Standards New Zealand, Wellington. *https://www.standards.govt.nz/sponsored-standards/building-standards/NZS1170-5*

Pekcan G, Mander JB and Chen SS. (1999). "Fundamental considerations for the design of non-linear viscous dampers". *Earthquake engineering & structural dynamics*, **28**(11): 1405-1425. DOI: 10.1002/(SICI)1096-9845(199911)28:11<1405::AID-EQE875>3.0.CO;2-A

Priestley MNJ. (2002). "Direct displacement-based design of precast/prestressed concrete buildings". *PCI journal*, **47**(6): 66-79. DOI: 10.15554/pcij.11012002.66.79

Rodgers GW, Mander JB, Chase JG, Leach NC and Denmead CS. (2008a). "Spectral analysis and design approach for high force-to-volume extrusion damper-based structural energy dissipation". *Earthquake Engineering & Structural Dynamics*, **37**(2): 207-223. DOI: 10.1002/eqe.752

Rodgers GW, Solberg KM, Chase JG, Mander JB, Bradley BA, Dhakal RP and Li L. (2008b). "Performance of a damage-protected beam-column subassembly utilizing external HF2V energy dissipation devices". *Earthquake Engineering & Structural Dynamics*, 37(13): 1549-1564. DOI: 10.1002/eqe.830

Rodgers GW. (2009). *"Next Generation Structural Technologies: Implementing High Force-to-Volume Energy Absorbers"*. Doctor of Philosophy Thesis, *University of Canterbury, Christchurch, New Zealand*. DOI: 10.26021/1363